21 September 1979, Volume 205, Number 4412 SCIENCE

Catalysis by Small Metal Clusters

Size-dependent catalytic activity can be correlated with changes in physical properties.

J. F. Hamilton and R. C. Baetzold

Summary. Experimental and theoretical studies of small clusters of metal atoms are aimed at revealing how properties change in the ultrafinely divided state. Thermodynamic, electronic, and structural features can be size-dependent and may be involved in determining the activity of small-particle catalysts. Correlations between these properties give indications of the features important in catalysis.

Several obvious and many less obvious changes in properties occur as metal atoms combine to form dimers, trimers, larger clusters, and so on, until finally a size is reached at which the collection is identifiable in every way as the bulk metal. Questions of fundamental importance have to do with the nature of the evolution of bulk metallic properties. Over what size range are properties intermediate between those of the atomic and metallic states? Is the transition abrupt or gradual, monotonic or discontinuous? Do all properties change in parallel fashion? Is the nature of the change the same for all metals, or does each have its own pattern? These and similar questions, although of great technological as well as fundamental interest, have remained intractable for many years. Modern analytical techniques—principally the experimental tools of surface analysis and the improved semiempirical computational techniques—have provided new approaches to these questions, and significant inroads to the difficult field are being made.

Technological Importance

The photographic process. Our interest has been attracted to this subject because of its relevance to the photographic process (*1*). The few photons striking a silver halide crystal in either black-and-white or color film produce a small cluster of silver atoms on the surface of the silver halide. Upon reaching the necessary size, this silver cluster acquires catalytic properties and can trigger the reduction of the entire crystal to silver by the reducing agent of the developer. Various photographic experiments give indirect evidence that the cluster, called a latent-image center, becomes catalytic rather abruptly, at a size of a few atoms, but that thermodynamic stability does not require as large a cluster. One wonders, of course, what more fundamental property it is that determines the catalytic activity. Are factors involved that can, in principle, be controlled, to optimize the process?

Heterogeneous catalysis. Similar, although not identical, questions apply to the finely divided metal catalysts used for petroleum refining, automobile-exhaust conversion, and chemical synthesis in general. The catalysts used are frequently precious metals, and it is important, in the interest of economy, to maximize the available surface by producing particles as small as possible. Over and above this straightforward dependence on surface area, however, more pronounced size effects are sometimes noted (*2*). For certain classes of chemical reactions, termed demanding reactions, the catalytic activity of smaller particles is different—frequently much higher—from that of larger particles, and much effort has been spent in attempts to stabilize the very smallest possible clusters. In these applications as well, knowledge of the reason for the high activity might hold the key to improvements in the process.

Method of Preparation

Over the past several years, we have been investigating the questions discussed above in an experimental program closely linked with theoretical calculations.

Small metallic clusters are formed on planar amorphous substrates (carbon, SiO_2, Al_2O_3, and so on) by vacuum deposition (*3*). In the earliest stages of formation, such deposits form discrete clusters, which eventually fuse to form continuous films but only at mean thicknesses of tens of monolayers. On these substrates the earlier stages of the condensation produce particles with a nearly random size distribution, whose mean size increases with deposit thickness. Figure 1 shows a family of curves giving the logarithm of the surface density of particles of size i or larger as a function of the logarithm of the mean thickness. At particle densities well below the saturation value, each curve is linear with slope i.

These relationships have been derived by an extrapolation, based on a model of the condensation mechanism, of size data obtained from transmission electron micrographs such as that shown in Fig. 2. The general form of the relationship applies at least to the group IB noble metals and the platinum-group metals of group VIII, and probably others as well.

The authors are in the Chemistry Division of the Research Laboratories, Eastman Kodak Company, Rochester, New York 14650.

0036-8075/79/0921-1213$01.75/0 Copyright © 1979 AAAS

Chemical Characterization

The classic problem of bridging the gap between the "clean" world studied by surface analysis in ultrahigh vacuum and the "real" world of a cluster or metal surface in the ambient or reacting environment is continually present. In this connection, Auger electron spectroscopy (AES) and photoelectron spectroscopy (PES) have been useful in characterizing the surface composition of the metal clusters (*4*). Most typical metal deposits such as silver adsorb significant amounts of sulfur, oxygen, carbon and sometimes chlorine after a few minutes of exposure to the atmosphere. For comparison, the techniques have been adapted to prepare clean metal deposits within the ultrahigh vacuum of the spectrometers (*4*, *5*) for studies of the clean surfaces in situ. Studies of the controlled adsorption of CO on palladium clusters of this type have also been reported (*6*).

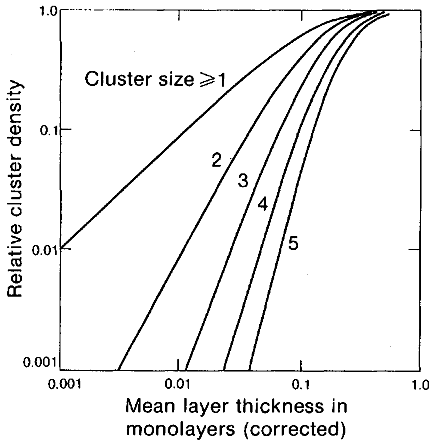

Fig. 1. Typical curves of log-normalized surface density of clusters of size *i* atoms or larger plotted against log-nominal thickness (corrected for volume diffusion) in monolayers of a vacuum deposit.

We have also probed the interaction between metal deposits and the carbon film supports (*4*). This interaction may be studied with AES because of the relatively shallow depth analyzed (≈ 10 angstroms) and the known sensitivity of the carbon *KLL* spectrum to oxidation state. Carbide and graphite forms of carbon have different spectral shapes, as illustrated by Fig. 3, which shows two coverages of iron on carbon. At low coverage (~ 8.0×10^{14} atoms per square centimeter) the carbon spectrum is like that of graphite, whereas at greater coverage (~ 1.0×10^{16} atoms per square centimeter) a carbide spectrum is obtained. The iron spectrum is unchanged. We attribute this effect to reaction of the iron with carbon and the associated electron transfer. A similar effect is observed for aluminum deposits but not for gold, silver, copper, or palladium. These experiments indicate that some metals, but not others, react with the support.

Deposits of this type have been used to study the size dependence of catalytic activity for certain chemical reactions, as well as the changes in electronic and structural properties. Promising correlations are beginning to emerge.

Catalytic Activity

We have investigated catalyzed oxidation-reduction reactions in the solution phase that are analogous to the reactions in the photographic development process: the reduction of silver ions to silver metal (*7*), the reduction of nickel or copper ions to the corresponding metal (*8*) [in processes known as "electroless plating" (*9*)], and the formation of formazan dyes from oxidative precursors (*10*). In each case it is possible to determine a minimum metal coverage and usually a minimum cluster size required for the catalyst.

For example, in the closest analog to photographic development, the reduction of silver ion in solution to metallic silver, the catalytic effectiveness of small gold clusters has been compared with that of silver clusters (*7*). A deposit of the clusters with some specified coverage is immersed in the reacting solution. Of the clusters over the distribution of sizes, only those large enough to act as catalysts have any effect. Silver is deposited on these particles, causing them to be enlarged until, after some appropriate time, they are easily distinguishable by electron microscopy. A count of the enlarged particles gives the surface density of particles above the minimum catalytic size.

The data collected in this way are then compared with the family of curves of Fig. 1 in the manner illustrated in Fig. 4. The data for silver catalyst clusters in Fig. 4 fit best to the curve for four or more atoms, whereas the gold clusters appear to be effective at the two-atom size. Gold is frequently used in small quantities as a sensitizer for photographic emulsions, and the photographic results strongly suggest that the gold is incorporated in the latent-image centers, rendering them more easily developable (*1*).

Another class of reactions that are similar to those in photographic development are involved in the commercial process known as electroless deposition. These reactions include the catalytic reduction of nickel ion in solution by hypo-

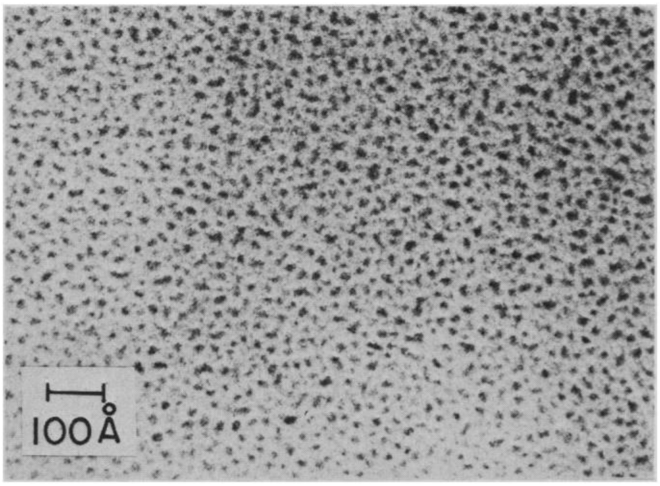

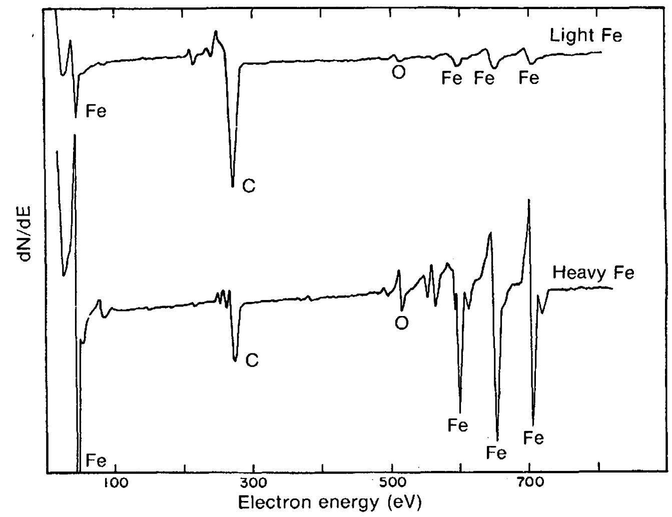

Fig. 2 (left). Electron micrograph of a deposit of iridium on carbon; the nominal thickness is 0.2 monolayer (magnification, $\times 10^6$; 1 mm = 10Å). Fig. 3 (right). Auger derivative spectra showing two coverages of evaporated iron on carbon (8×10^{14} and 1×10^{16} atoms per square centimeter).

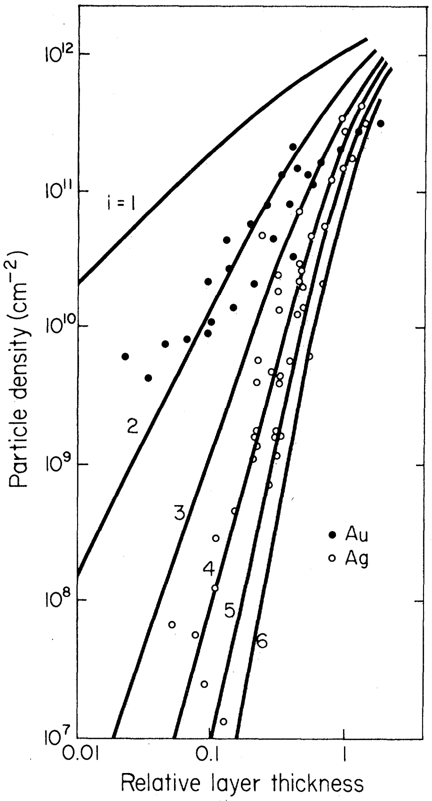

Fig. 4. Data indicating the surface density of catalytic clusters of silver (○) and gold (●) for reduction of silver ion from aqueous solution. Curves are those from Fig. 1.

phosphite or amine borane reducing agents, forming metallic nickel (*8*), and the catalytic reduction of tetrazolium salts to insoluble formazan dyes by similar reducing agents (*10*). The preferred catalysts are the platinum group metals, particularly palladium. In either case, an insoluble product is formed at the initial catalyst site. Isolated films of either product, after equilibration in the atmosphere, are found to be inactive as catalysts. The question therefore arises whether the initial palladium catalyst diffuses through the depositing film to maintain contact with the solution, or is buried under the layers of reaction product.

To answer this question for both reactions, AES has been used in connection with argon sputter-ion etching (*11*). This technique permits continuous analysis while the film is being etched away at a constant rate (~ 50 Å per minute). As shown in Fig. 5 for nickel films, no palladium is detected on the surface, but a small signal due to palladium appears when about 2700 Å of the film has been etched away. Note that the nickel deposit is about 3600 Å thick and that as it is removed, signals due to carbon, silicon, and oxygen from the support begin to appear. Contaminants of sulfur, chlorine, and carbon are also present throughout the nickel film. Since it is unlikely that the palladium can exert a long-range effect on the surface of the nickel film, we must conclude that the fresh nickel film is autocatalytic.

For the nickel-reduction reaction it is possible to determine not only that there is a minimum size for the catalyst clusters (*8*) but also that some anomalies occur as the particles become larger (*12*, *13*). Palladium continues to be an equally effective catalyst even for continuous films, but platinum, rhodium, and iridium all show a complete loss of activity at sizes between 10 and 20 Å in diameter. The effect is demonstrated for platinum in Fig. 6.

Origin of Size Effects

Until very recently, suggestions about the causes of such particle size effects on catalytic activity have been very speculative and have differed widely. Some workers have given interpretations in terms of the thermodynamic properties, using a Gibbs-Thomson analysis (*14*, *15*). Others have relied heavily on discussions of localized geometry and bonding modes, reasoning that low-coordination sites are more common on small clusters than on more nearly ideal surfaces (*16*). Structural forms other than elements of the bulk crystal lattice, such as polytetrahedral arrangements, have been predicted for small clusters (*17*) and indeed have been observed for some metals (*18*). Some such structures can give rise to bonding sites not common on larger crystallites.

Still other proposals to explain particle size effects have to do with the collective electronic structure of the cluster (*19*). As atoms combine to grow toward the bulk metal, electronic levels can shift and split, symmetry effects can change in importance, bands form and broaden, and orbital occupancy may change significantly. These changes can clearly influence the interactions with molecules in the surroundings.

Experimental Studies

Thermodynamic properties. Vapor-deposited clusters provide a useful format for studying some of these properties. Silver particles in the range 10 to 100 Å in equilibrium with a solution of silver ions have been studied by Malinowski and colleagues (*14*). The behavior agrees with Gibbs-Thomson concepts: smaller particles dissolve and larger ones grow, and the transition size is related to the ionic strength and redox potential of the solution. Data are interpretable in terms of a fixed surface energy.

Electronic properties. The techniques of AES and PES have been used to probe the density of occupied states in clusters of various sizes. The change from a set of electronic levels to a spectrum characteristic of bulk metal is gradual, and the spectrum becomes indistinguishable from that of bulk only when particles contain about 100 atoms. For example, gold shows changes in the Auger valence (*NOO*) transitions as a function of particle size. In this example the relative separation between peaks changes 4 electron volts between the atom and bulk size with the shift essentially complete in particles of 100 atoms (*4*).

X-ray photoelectron spectra (*5*, *12*, *13*, *20*) from silver, gold, and the platinum-group metals show that the *d* bandwidth broadens and the ionization threshold decreases with increasing cluster size. Typical results are shown in Fig. 7. Differences from bulk properties vanish only when cluster sizes of 50 to 100 atoms are attained. This type of measurement

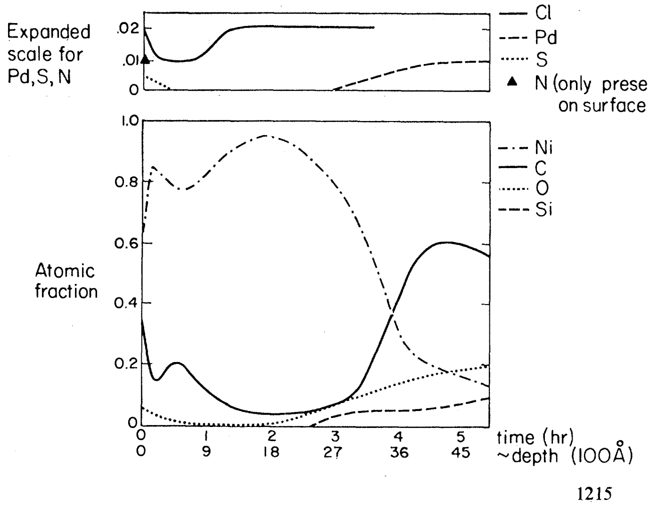

Fig. 5. Depth profile of nickel film showing the atomic fraction of the element present, estimated by AES, plotted against the depth of material ion-etched away.

and the AES data discussed for gold are in good agreement as to the size for saturation of these *d*-band properties.

For the platinum-group metals, a rather impressive correlation has been found between the electronic structure and the catalytic activity for nickel reduction (*5*, *13*). In the small-cluster size range, where all four metals are active catalysts, the density-of-states function is consistent with a $d^{n-1}s^1$ electronic configuration, whereas in the bulk metals the *d* levels are more nearly filled. The transition is most clearly revealed by high-resolution scans of the high-energy edge of the *d* band, as shown for platinum in Fig. 8. At the larger particle size, the sharpness of the edge is limited only by instrument resolution, whereas for the smaller particles, the gradient of the edge is distinctly lower. The difference is taken to indicate less complete occupancy of these states in the smaller particles.

The size range for the transition in electronic structure coincides with that at which the catalytic activity is lost. Furthermore, the transition particle size increases in the order iridium, rhodium, platinum, which parallels the order of increasing density of states at the Fermi level, $D(E_F)$, among these metals, palladium having an even higher density than platinum.

There is probably some charge exchange with the substrate in these samples, and the same pattern of behavior may not occur on isolated clusters or even those on markedly different supports. Even if the details are not universal, however, the correlation between electronic structure and catalytic activity is no less impressive for these preparations, allowing a strong argument to be made that changes in the number of unoccupied *d* states and in $D(E_F)$ are responsible for the reported size effects.

These particular features of the electronic structure have been discussed repeatedly as important factors in catalysis of certain reactions (*21*). The reasoning is that covalent bonds with reactant molecules involve electron sharing principally in the *d* electronic levels of the catalyst, owing to their localized nature. Both the bond strength and the rate of bonding are believed to increase with the number of vacant *d* states, which in turn is greater when $D(E_F)$ is high. Evidence for the importance of these factors has come from correlations between the rates of catalyzed reactions and the number of *d* holes in bulk metals and alloys. To our knowledge, the experiments described represent the first demonstration of the involvement of these same concepts in particle size effects.

Structure. What is not known yet is whether there is also a change in geometric structure in the same size range. If so, there may be a cause-and-effect relationship between the electronic change and a structural change, and the electronic versus structural argument for catalytic activity would be moot.

The particle size range in question appears to be one for which structural information may be obtained by either electron diffraction or extended x-ray absorption fine structure (EXAFS) or both. Careful Fourier analysis of background-corrected electron diffraction patterns has been used to distinguish polytetrahedral or multiple-twinned structures from bulk cubic forms of rare gas clusters in the vapor phase (*22*) and of some metal deposits near this size range (*23*). Interpretations are not always unambiguous, but the method holds some promise.

The EXAFS results should be more definite, provided the sensitivity is adequate and some uncertainties about phase corrections and dynamic disorder can be understood. Initial experiments (*24*) have been done on copper and nickel clusters, and typical data are shown in Fig. 9. Some structural conclusions can be stated at this time. The data on nearest-neighbor distance indicate a contraction at small sizes, approaching separations reported for the dimers in each case. The spectra are not yet good enough to obtain a complete radial distribution, which would reveal other structural details as well.

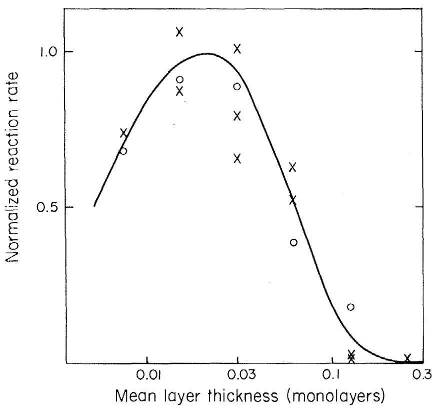

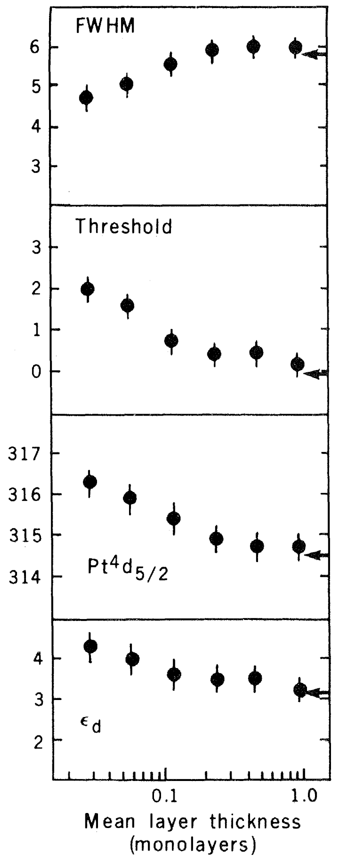

Fig. 6 (above). Normalized reaction rate for Ni^{2+} reduction from solution plotted against mean layer thickness for platinum cluster catalysts. Fig. 7 (right). Variation of valence-band width [full width at half-maximum (*FWHM*)], low-binding-energy valence-band edge (threshold), core-level binding energy ($^4d_{5/2}$), and valence-band centroid (ϵ_d) with platinum mean layer thickness. Bulk values are given by arrows.

Stepped Surfaces

Another approach in attempting to distinguish between effects of surface structural configuration and electronic effects due to finite size lies in the study of deliberately stepped surfaces of large crystals. The analogy between adsorption sites on small clusters and stepped surfaces has been advocated particularly by Somorjai and co-workers (*25*), who introduced the concepts some years ago and have found kinetic evidence to support the claim (*26, 27*). On these surfaces there are atoms with low coordination numbers which are not affected by the electronic perturbations associated with a cluster of limited size.

Chemisorption on stepped and low-index surfaces of silver has been studied by low-energy electron diffraction (LEED). This technique is useful for such studies since the elastically scattered electrons are diffracted from ordered surface structures. As an example, the LEED pattern resulting from a stepped surface of silver consists of split spots arranged in a hexagonal pattern. A surface such as [3(111) × (100)], in the notation of Somorjai, consists of terraces containing three rows of atoms in the (111) orientation separated by steps one atom high with the (100) orientation. A number of gases including O_2, C_2H_4, and Cl_2 have been chemisorbed at room temperature on this surface and on the (111) surface of silver, which lacks steps. With C_2H_4, no ordered adsorption on the stepped surface takes place, as evidenced by an unchanged spot pattern. A somewhat higher background is observed after C_2H_4 exposure, indicating perhaps some disordered adsorption. Similar effects are found on the (111) surface. A more spectacular effect occurs upon aging the stepped surface overnight in the spectrometer.

After the stepped surface has aged, the pattern of the (111) surface appears, and AES confirms the presence of small sulfur, oxygen, and carbon impurities on the surface. Cleaning and annealing cause the pattern to revert to that of the stepped surface. Apparently, low levels of impurities are responsible for the motion of surface atoms to form extended (111) areas on the silver surface which are larger than the coherence diameter of the spectrometer (200 to 500 Å). This is a surprisingly high mobility of atoms and indicates the sensitivity of surface structure to environment. Such effects should be important in catalysis by small metal particles and are similar to the rearrangements recently reported by Blakely and Somorjai (*28*) for platinum surfaces.

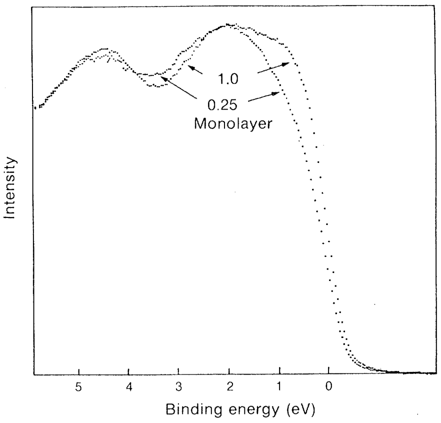

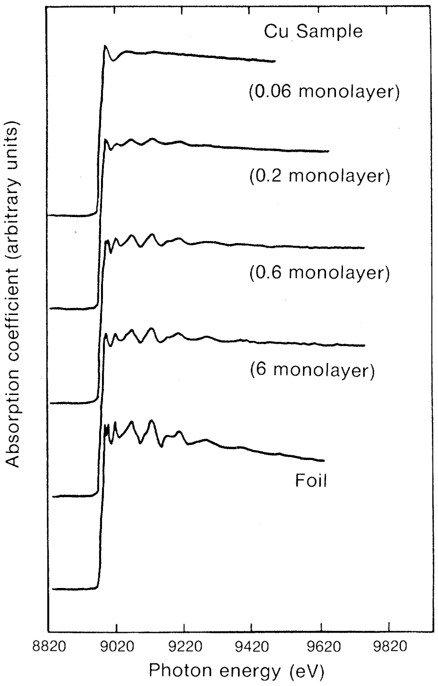

Fig. 8 (above). High-resolution spectra of valence-band edge for platinum clusters of two sizes. Fig. 9 (right). X-ray absorption spectra at the *L* edge for copper clusters of various mean layer thicknesses. The EXAFS structure on the high-energy side of the edge becomes more pronounced as the cluster size increases.

Calculations

We began a study of the electronic properties of small metal particles in 1970, using molecular orbital theory to better understand the relationship between cluster size and electronic properties. Throughout these studies we have benefited greatly from the advice of Roald Hoffmann, who has maintained an active interest in this area. We employ the extended Hückel (EH) (*29*) and complete neglect of differential overlap (CNDO) (*30*) methods in this work. These methods are useful for perceiving cause-and-effect relationships without becoming involved in a great degree of complexity. We have also found that they accurately predict trends and values of a number of quantities before experimental measurement. A number of these cases will be discussed. Our primary goal has been the prediction of trends and effects rather than the precise calculation of some particular variable. A recent review (*31*) of clusters and surfaces provides a comprehensive overview of various types of calculations that have been applied to this problem.

Semiempirical molecular orbital theory can be criticized on the grounds that a parameter choice is involved in its application. It should be pointed out, however, that some form of parameter choice is also involved in most methods of present-day calculation. This may involve basis set selection in ab initio calculations, sphere radii or alpha coefficients in $X\alpha$ calculations, or ionization potential and orbital exponents in EH calculations. In these EH calculations, orbital exponents are taken from atomic Hartree-Fock calculations (*32*), and ionization potentials are derived from tables of atomic spectra (*33*).

Silver and copper. The binding energy per atom of a metal cluster is determined by calculating the energy as a function of bond length for various assumed geometries. We have found that the small neutral clusters of silver and copper prefer a linear as opposed to a two-dimensional or three-dimensional structure (*34*). The bonding orbitals of silver (copper) are primarily the $5s$ ($4s$), although hybridization with the $5p$ ($4p$) and $4d$ ($3d$) orbitals definitely takes place. A recent ab initio calculation (*35*) supports these geometric findings for small copper clusters. This geometric effect may be understood in terms of the antibonding $4s$ molecular orbitals, which are occupied in the neutral cluster and are destabilized in high-symmetry structures. In addition to this geometric effect, we note that the binding energy per atom increases with cluster size, but that there is an oscillation leading to relatively greater stability at even-sized rather than odd-sized neutral clusters. The equilibrium bond length calculated for these clusters shows an elongation with increasing size. This effect is also traced to the antibonding orbitals, which become occupied in the larger clusters to a greater extent.

The ionization potential (IP) and electron affinity (EA) of the silver clusters vary as a function of cluster size. This behavior is shown for three-dimensional clusters of silver in Fig. 10 (a cluster of 3 atoms is a triangle; 4, a tetrahedron; 5, a bipyramid; 6, a square bipyramid; 7, a bicapped pentagon; 8, a cube; and 9 and larger, a face-centered cubic structure). The IP decreases as size increases, whereas the EA increases as size increases, and these quantities tend to converge as would be expected for the bulk metal. There is, however, a sizable difference between IP and EA at 13 atoms, providing a considerable deviation from bulk properties. Oscillations in stability, similar to the ones described earlier for linear structures, are noted in Fig. 10 for three-dimensional structures. This is caused by the relatively greater stability of closed-shell than open-shell configurations in CNDO. These effects are also observed in EH calculations, where the point of convergence of IP and EA (bulk work function) is shown to be dependent on geometry. Linear clusters have a calculated work function 1.5 eV larger than that of three-dimensional face-centered cubic clusters.

Extended Hückel calculations show that the IP of silver clusters decreases from 8.60 eV for Ag_2 to 6.17 eV for the bulk (*36*). This decrease of 2.4 eV is a consequence of the spreading of the 5*s* band and the occupation of antibonding states in the larger clusters. This effect is in accord with ionization threshold measurements by ESCA (electron spectroscopy for chemical analysis) for silver clusters on carbon film (*5*). As size increases the threshold decreases 2.5 eV, moving toward the vacuum level, in close accord with our calculation. In addition to this effect, the odd-even oscillations reported earlier for silver clusters have been observed in experiments. These include IP measurements on sodium clusters (*37*) and secondary-ion mass spectrometry measurements on silver anion clusters (*38*).

The occupied density of states calculated for the valence orbitals of silver clusters is shown in Fig. 11. The molecular orbitals obtained from the noniterative EH calculation are broadened by a Gaussian and a lifetime function to simulate experimental density-of-states curves. Although we note certain similarities between the 13-atom cluster and bulk densities of states, considerable changes occur as size increases, particularly when clusters having incomplete shells of nearest neighbors are considered (for example, 39 atoms). Small clusters in the size range considered here have not attained a bulk density of states. The portions of Fig. 11 having most intensity comprise *d* orbitals, whereas the *s* orbitals lie on the low-energy side of these peaks. The bulk calculation for silver bears strong similarity to the density of states calculated by solid-state physics techniques, such as the augmented-plane-wave method (*39*). The two curves are similar in shape and in the position of portions of the spectrum relative to the Fermi energy. The largest clusters containing 39 atoms do not possess the bulk *d* bandwidth, but other EH calculations (*20*) show that 85 to 90 percent of the bulk *d* bandwidth is attained at 79 atoms.

Table 1. Comparison of calculated and observed (*40*) values of the energy gap (ΔE) between the highest occupied molecular orbital and the lowest unoccupied molecular orbital for silver clusters in low-temperature matrices.

Cluster	ΔE (nm)	
	Observed	Calculated
Ag_2	387, 412	404
Ag_3	440	489
Ag_4	490	517
Ag_5	505	581
Ag_6	520	664
Ag_7	536	800

Thus we conclude that rather large clusters, having about 100 atoms or more, are required to achieve essentially bulk bandwidths. From our reported IP and energy-gap calculations (*36*), this size is also required for convergence of the latter properties to bulk values.

The energy gap between highest occupied molecular orbital (HOMO) and lowest unoccupied molecular orbital (LUMO) is a measure of the first optical transition in small clusters. Our calculations show that this gap decreases with increasing size of the cluster, as is true for silver and copper clusters. Recently, Ozin and Huber (*40*) measured this quantity for silver clusters in low-temperature matrices, and their data are shown in Table 1 along with our calculated values. Clearly the trends agree, and the calculated values are not too far from the experimental values. The deviations at larger sizes may be due to the fact that HOMO-LUMO gaps do not necessarily correspond to transition energies, owing to intensity considerations.

Palladium. Palladium clusters offer some interesting contrasts to the silver and copper clusters discussed earlier. The atomic electron configuration is $4d^{10}$, so we are dealing with closed shells. The bonding in palladium clusters is due, for the most part, to the 5*s* orbitals, which overlap strongly and form a molecular orbital that is more strongly bonding than the 4*d* molecular orbitals and leads to a $4d^{9}5s^{1}$ configuration in Pd_2. This configuration approaches $4d^{9.4}5s^{0.6}$ at eight to ten atoms, where only minor changes take place with size increases. This electron configuration compares favorably with the value $4d^{9.6}5s^{0.4}$ determined from bulk experimental measurements on palladium (*41*). The odd-even oscillations in IP, EA, and binding energy of silver and copper clusters are not found for palladium clusters.

The local density of states shows some interesting effects that are dependent on coordination number (*42*). For clusters having incomplete outer shells of atoms, the density of states at the Fermi energy is largest for atoms with a coordination number of 7 to 9. Atoms having fewer or more nearest neighbors exhibit a smaller

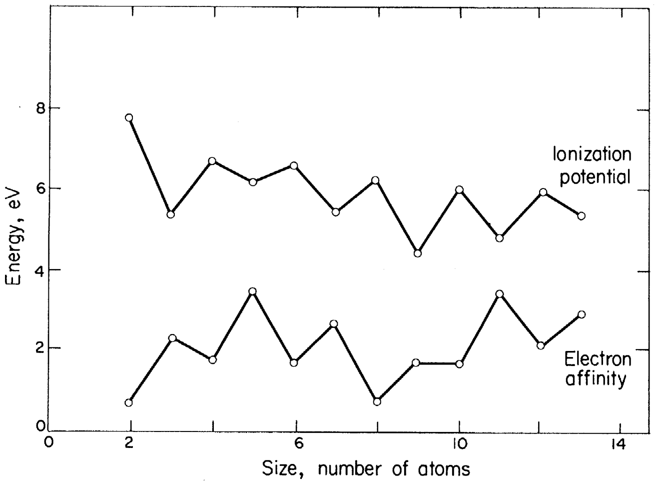

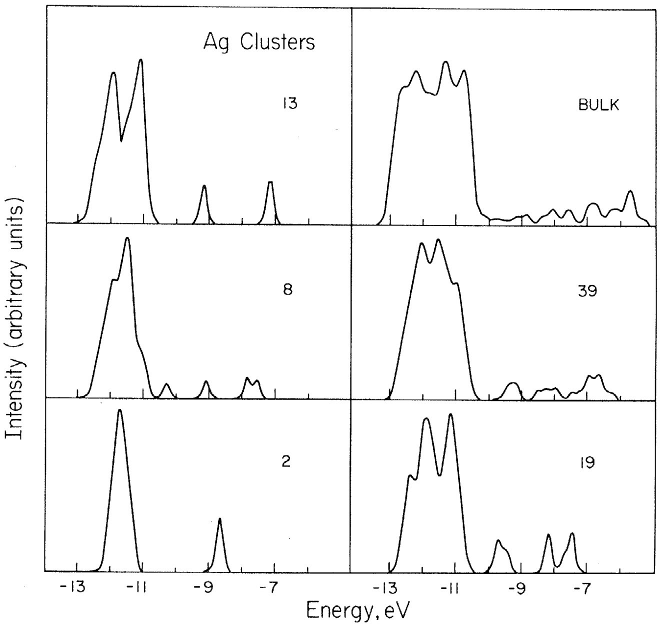

Fig. 10 (left). Ionization potential and electron affinity of three-dimensional silver clusters calculated by CNDO. Fig. 11 (right). Occupied density of states for various-sized silver clusters compared with the bulk property.

$D(E_F)$. Such a variation in small clusters may point to an electronic effect related to site geometry. These effects could play an important role in bonding of molecules and catalysis and may in some way be related to the experimental effects on stepped surfaces that Somorjai reported (*26*).

The cause of the high $D(E_F)$ for atoms of intermediate coordination can be traced to a balance between surface potential and band-broadening effects. Positive charges build up on atoms of high coordination because their projected density of states is spread over a greater energy range as a result of more nearest neighbors. Thus a relatively greater fraction of states lies above the Fermi energy and is unoccupied. Opposing this separation of charge, a surface potential develops that shifts orbitals on surface atoms about 1 eV closer to the vacuum level relative to bulk. We calculate this shift in potential to be 0.89 eV for *s* electrons and 1.75 eV for *d* electrons in a fully symmetric Pd_{19} cluster. These opposing forces lead to a positioning of orbitals on atoms with intermediate coordination near the Fermi energy. This particular balance achieved for palladium clusters does not necessarily lead to the same $D(E_F)$ behavior for other elements.

Photographic Models

Models for the photolytic formation of silver clusters in silver bromide are very important in planning and interpreting photographic experiments. In the Gurney-Mott model (*43*), the silver clusters that are the latent-image centers grow by alternating photoelectron and interstitial silver ion trapping at a site in the crystal. We have modeled latent-image formation by using CNDO methods to calculate electronic properties of silver clusters adsorbed to a small silver bromide support (*44*).

Silver atoms are placed successively on a 14-ion model of the silver bromide support. Relaxation of the atoms to their equilibrium position is allowed, but the ions are fixed in the lattice position. This small model for the semiconductor is simplified in many respects, but it provides the neighboring ions to the cluster to treat this interaction.

A donation of electron charge from silver atom to silver bromide support is found in our calculation. The magnitude to this charge varies with the geometry of the site of adsorption but is about 0.5 for one atom. This partial positive charge remains on larger clusters and makes them similar to cations. The electron affinity and ionization potential of the adsorbed clusters may be compared with the calculated values for the silver bromide support to obtain the values shown in Fig. 12. This is a plot on a relative energy scale which shows the stability of neutral and anionic clusters with respect to loss of an electron to the conduction band. These data show that the neutral clusters are stable, but that Ag_2^- is unstable by 0.02 eV with respect to this process. Thus, such a species would be short-lived and would require capture of a silver ion for stabilization. The other neutral clusters could capture photoelectrons which would make it coulombically favorable for them to capture an interstitial silver ion. These effects are due in part to the partial positive charge which we find on the small adsorbed silver clusters, and this charge should extend to larger silver bromide models. The picture that evolves from the CNDO calculations is in close accord with models derived from coulombic considerations (*45*).

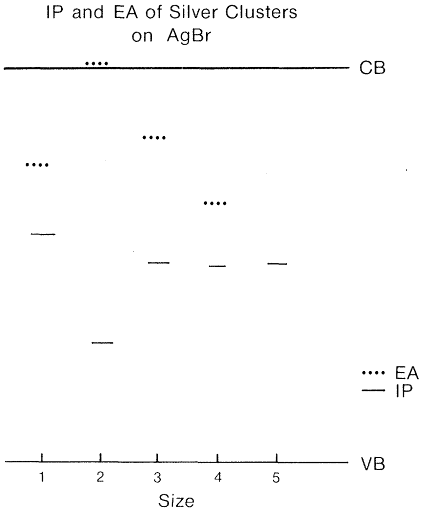

Fig. 12. Ionization potential and electron affinity for adsorbed silver clusters compared with the silver bromide conduction band (*CB*) and valence band (*VB*).

Conclusion

The questions we posed in the introduction have many facets, and full answers will require the collection of a large body of experimental and theoretical evidence. Many academic and industrial laboratories worldwide have devised their own approaches to these questions, however, and there is reason to expect that a period of improved understanding lies not too far ahead. The importance of optimizing catalyst performance to the problems of energy conservation, productivity, raw-stock diversification, and innovation, coupled with the empirical nature of the whole history of the practice, makes it almost certain that technological advance will accompany increased understanding.

References and Notes

1. T. H. James, Ed., *The Theory of the Photographic Process* (Macmillan, New York, ed. 4, 1977).
2. M. Boudart, A. Aldag, J. E. Benson, N. A. Dougharty, C. G. Harkins, *J. Catal.* **6**, 92 (1966); J. R. Anderson and R. J. MacDonald, *ibid.* **19**, 227 (1970); J. R. Anderson, R. J. MacDonald, Y. Shimoyama, *ibid.* **20**, 147 (1971); P. B. Wells, *Surface and Defect Properties of Solids* (Proceedings of the Fifth International Conference, Miami, 1972) (Chemical Society, London, 1972), vol. 1, chap. 9; R. A. Dalla Betta and M. Boudart, in *Catalysis*, J. W. Hightower, Ed. (North-Holland, Amsterdam, 1973), p. 1329; T. E. Whyte, Jr., *Catal. Rev.* **8**, 117 (1973); G. C. Bond, *Platinum Met. Rev.* **19**, 126 (1975); M. A. Vannice, *J. Catal.* **40**, 129 (1975); J.-M. Dartigues, A. Chamberlan, F. G. Gault, *J. Am. Chem. Soc.* **98**, 856 (1976).
3. J. F. Hamilton and P. C. Logel, *Thin Solid Films* **16**, 49 (1973); *ibid.* **23**, 89 (1974); ———, R. C. Baetzold, *ibid.* **32**, 233 (1976).
4. R. C. Baetzold, *J. Appl. Phys.* **47**, 3799 (1976).
5. M. G. Mason, L. J. Gerenser, S.-T. Lee, *Phys. Rev. Lett.* **39**, 288 (1977).
6. R. Unwin and A. M. Bradshaw, *Chem. Phys. Lett.* **58**, 58 (1978); M. Grunze, *ibid.*, p. 409.
7. J. F. Hamilton and P. C. Logel, *Photogr. Sci. Eng.* **18**, 507 (1974).
8. ———, *J. Catal.* **29**, 253 (1973); J. F. Hamilton, *J. Vac. Sci. Technol.* **13**, 319 (1976); *J. Phys. (Paris)* **38**, C2-181 (1977); M. Lelental, *J. Electrochem. Soc.* **120**, 1651 (1973); *ibid.* **122**, 486 (1975); *J. Catal.* **32**, 429 (1974).
9. E. B. Saubestre, *Met. Finish.* **60** (No. 6), 67 (1962); *ibid.* (No. 7), p. 49; *ibid.* (No. 8), p. 45; *ibid.* (No. 9), p. 59; W. Goldie, *Metallic Coating of Plastics* (Electrochemical Publications, Middlesex, 1968); J. Thewlis, in *Encyclopaedic Dictionary of Physics* (Pergamon, Oxford, 1971), suppl. vol. 4, p. 277.
10. M. Lelental and H. Gysling, *J. Photogr. Sci.* **26**, 135 (1978).
11. R. C. Baetzold and R. E. Mack, *J. Catal.* **37**, 251 (1975).
12. M. G. Mason and R. C. Baetzold, *J. Chem. Phys.* **64**, 271 (1976).
13. M. G. Mason, J. F. Hamilton, S.-T. Lee, B. F. Nellis, L. J. Gerenser, P. C. Logel, unpublished results.
14. I. Konstantinov, A. Panov, J. Malinowski, *J. Photogr. Sci.* **21**, 250 (1973); I. Konstantinov and J. Malinowski, *ibid.* **23**, 1 and 145 (1975).
15. P. J. Hillson, *ibid.* **22**, 31 (1974); *ibid.* **23**, 15 (1975).
16. O. M. Poltorak and V. S. Boronin, *Russ. J. Phys. Chem.* **40**, 1436 (1966); R. Van Hardeveld and A. Van Montfoort, *Surf. Sci.* **4**, 396 (1966); R. Van Hardeveld and F. Hartog, *ibid.* **15**, 189 (1969).
17. M. R. Hoare and P. Pal, *Adv. Phys.* **20**, 161 (1971); *ibid.* **24**, 645 (1975); C. L. Briant and J. J. Burton, *J. Chem. Phys.* **63**, 204 (1975); C. L. Briant, *Faraday Discuss. Chem. Soc.* **61**, 25 (1976).
18. T. Komoda, *Jpn. J. Appl. Phys.* **7**, 27 (1968); N. R. Avery and J. V. Sanders, *J. Catal.* **18**, 129 (1970); D. Watanabe and R. Miida, *Jpn. J. Appl. Phys.* **11**, 296 (1972); M. Gillet, *Surf. Sci.* **67**, 139 (1977).
19. R. Kubo, *J. Phys. Soc. Jpn.* **17**, 975 (1962); L. P. Gor'kov and G. M. Eliashberg, *Sov. Phys. JETP* **21**, 940 (1965); R. Denton, B. Miihlschlegel, D. J. Scalapino, *Phys. Rev. Lett.* **26**, 707 (1971); *Phys. Rev. B* **7**, 3589 (1973).
20. M. G. Mason, J. F. Hamilton, R. C. Baetzold, unpublished results.
21. D. A. Dowden, *J. Chem. Soc.* (1950), p. 242; P. W. Reynolds, *ibid.*, p. 265; A. Clark, *The Theory of Adsorption and Catalysis* (Academic Press, New York, 1970); *The Chemisorptive Bond* (Academic Press, New York, 1974); L. H. Bennett, A. J. McAlister, J. R. Cuthill, N. E. Erickson, R. E. Watson, *J. Mol. Catal.*, **2** 203 (1977); P. B. Wells, in *Proceedings of the Symposium on Electrocatalysis*, M. W. Breiter, Ed. (Electrochemical Society, Princeton, N.J., 1974), p. 1.

22. J. Farges, B. Raoult, G. Torchet, *J. Chem. Phys.* **59**, 3454 (1973); J. Farges, *J. Cryst. Growth* **31**, 79 (1975).
23. H. Morimoto, *J. Phys. Soc. Jpn.* **13**, 1015 (1958); ——— and H. Sakata, *ibid.* **17**, 136 (1962); D. Watanabe and R. Miida, in (*18*); A. Yokozeki, *J. Chem. Phys.* **68**, 3766 (1978).
24. G. Apai, J. F. Hamilton, J. Stöhr, A. Thompson, *Phys. Rev. Lett.* **43**, 165 (1979).
25. B. Lang, R. W. Joyner, G. A. Somorjai, *Surf. Sci.* **30**, 454 (1972).
26. G. A. Somorjai, *Science* **201**, 489 (1978).
27. D. R. Kahn, E. C. Petersen, G. A. Somorjai, *J. Catal.* **34**, 294 (1974).
28. D. W. Blakely and G. A. Somorjai, *Surf. Sci.* **65**, 419 (1977).
29. R. Hoffmann, *J. Chem. Phys.* **39**, 137 (1963).
30. J. A. Pople, D. P. Santry, G. A. Segal, *ibid.* **43**, S129 (1965).
31. E. L. Muetterties, T. N. Rhodin, E. Band, C. F. Brucker, W. R. Pretzer, *Chem. Rev.* **79**, 91 (1979).
32. E. Clementi and D. L. Raimondi, *J. Chem. Phys.* **38**, 2686 (1963).
33. C. E. Moore, *Natl. Bur. Stand. (U.S.) Circ. 467* (1949).
34. R. C. Baetzold, *J. Chem. Phys.* **55**, 4363 (1971).
35. C. Bachmann, J. Demuynck, A. Veillard, *Gazz. Chim. Ital.* **108**, 389 (1978).
36. R. C. Baetzold, *J. Chem. Phys.* **68**, 555 (1978).
37. E. J. Robbins, R. E. Leckenby, P. Willis, *Adv. Phys.* **16**, 739 (1967).
38. G. Hortig and M. Mueller, *Z. Phys.* **221**, 119 (1969).
39. N. E. Christensen, *Phys. Status Solidi B* **54**, 551 (1972); A. Barrie and N. E. Christensen, *Phys. Rev. B* **14**, 2442 (1976).
40. G. A. Ozin and H. Huber, *Inorg. Chem.* **17**, 155 (1978).
41. F. W. Mueller and M. G. Priestley, *Phys. Rev.* **148**, 638 (1966); J. B. Ketterson, M. G. Priestley, J. J. Vuillemin, *Phys. Lett.* **20**, 452 (1966).
42. R. C. Baetzold, *J. Phys. Chem.* **82**, 738 (1978).
43. R. W. Gurney and N. F. Mott, *Proc. R. Soc. London Ser. A* **164**, 151 (1938).
44. R. C. Baetzold, *Photogr. Sci. Eng.* **19**, 11 (1975).
45. J. F. Hamilton and L. E. Brady, *ibid.* **8**, 189 (1964).

Psychotropic Drugs as Behavioral Teratogens

Charles V. Vorhees, Robert L. Brunner, Richard E. Butcher

Summary. Three psychotropic drugs were administered to pregnant rats and were then evaluated for their behavioral and reproductive effects in the offspring. Control rats received either saline or vitamin A. Prochlorperazine had the most disruptive effects on reproduction and growth, but had the least effect on behavior. Propoxyphene had no apparent effects on reproduction or growth, but produced a variety of behavioral changes. Fenfluramine was intermediate in its effects on reproduction and growth and had behavioral effects that were revealed in tests of preweaning development. The data suggest that systematic tests of behavior add important information to evaluations of reproductive toxicity that cannot, at present, be obtained by other means.

Prenatal exposure to certain drugs, such as thalidomide, and environmental agents, such as methylmercury, can cause abnormal embryonic development that results in major physical malformations, that is, teratogenesis. Recently, it has been recognized that some agents may also induce abnormalities in the behavioral capacities of offspring (*1*). Examples of such abnormalities are the fetal alcohol, fetal hydantoin, and fetal trimethadione syndromes (*2*), as well as long-term effects of fetal methadone or heroin withdrawal and of some medications used during labor and delivery (*3*). The agents causing these syndromes may be classified as behavioral teratogens.

The consequences of prenatal exposure to behavioral teratogens were recognized initially only through the accompanying physical abnormalities, or, in the case of medications used during labor, by their documented use during delivery. It is questionable whether a pure behavioral teratogen, unaccompanied by overt congenital malformations, could be successfully uncovered in the human population. Behavioral deficits are usually recognized only at school age, at which time it is too late to establish a causal relationship with drug administrations that might have occurred before birth. One solution would be to develop animal models that could be used for screening for the effects of drugs and other chemicals on behavior, in a manner similar to the screening systems that have been developed for teratogenesis, mutagenesis, and carcinogenesis.

In the study described here we used pregnant rats and their offspring to screen for the effects of three psychotropic drugs that are known to produce little or no structural teratogenicity even when administered at very high doses. We found that one of these drugs may fulfill the criteria for being a pure behavioral teratogen in rats. The three psychotropic drugs were prochlorperazine, fenfluramine, and propoxyphene. Prochlorperazine has been compared to other phenothiazines of the piperazine type (*4*). Prochlorperazine was shown to have low teratogenic activity when cleft palate was used as the index of abnormality. Fenfluramine is widely prescribed as an appetite depressant, but has recently been incriminated as a potential neurotoxin (*5*). Fenfluramine and propoxyphene have been shown to be nonteratogenic in rodents, rabbits, and monkeys, although limited clinical data suggest a link between propoxyphene and cleft palate in humans (*6*).

Adult Sprague-Dawley rats (Laboratory Supply, Indianapolis) were used for breeding. Males weighed about 400 grams and females about 260 grams at conception. The date of conception was determined by expelled vaginal plugs, and was considered day 0 of gestation. All females were primiparous. Daily on days 7 to 20 of gestation females were given, by stomach tube, one of the following: prochlorperazine edisylate (Pz, 25 milligrams per kilogram of body weight), fenfluramine hydrochloride (Ffl, 20 mg/kg), propoxyphene hydrochloride (Pp, 75 mg/kg), vitamin A palmitate (40,000 international units per kilogram, or 12 mg/kg), or saline. All drugs were given in saline in a volume of 5 milliliters per kilogram of body weight except vitamin A, which was solubilized with 12 percent sorethytan oleate and given in a volume of 1 ml/kg. Vitamin A was included in this study as a "positive" control or reference treatment because of its well-known adverse effects on behav-

Drs. Vorhees and Brunner are assistant professors and Dr. Butcher is associate professor of Research Pediatrics in the Behavioral Sciences Unit, Division of Inborn Errors of Metabolism, Children's Hospital Research Foundation and the University of Cincinnati College of Medicine, Cincinnati, Ohio 45229.

0036-8075/79/0921-1220$01.25/0 Copyright © 1979 AAAS